AD

TECHNICAL REPORT BRL-TR-2796

THE TWO PHASE FLOW SIMULATION OF LOVA PROPELLANT INTERIOR BALLISTIC BEHAVIOR USING THE XNOVAK CODE

G. E. KELLER
A. W. HORST

APRIL 7, 1987

US ARMY BALLISTIC RESEARCH LABORATORY
ABERDEEN PROVING GROUND, MARYLAND

Destroy this report when it is no longer needed.
Do not return it to the originator.

Additional copies of this report may be obtained from the National Technical Information Service, U. S. Department of Commerce, Springfield, Virginia 22161.

The findings in this report are not to be construed as an official Department of the Army position, unless so designated by other authorized documents.

The use of trade names or manufacturers' names in this report does not constitute indorsement of any commercial product.

UNCLASSIFIED
SECURITY CLASSIFICATION OF THIS PAGE A182 921

REPORT DOCUMENTATION PAGE

Form Approved
OMB No 0704-0188
Exp Date Jun 30, 1986

1a REPORT SECURITY CLASSIFICATION	1b. RESTRICTIVE MARKINGS
2a. SECURITY CLASSIFICATION AUTHORITY	3. DISTRIBUTION / AVAILABILITY OF REPORT
2b. DECLASSIFICATION / DOWNGRADING SCHEDULE	
4. PERFORMING ORGANIZATION REPORT NUMBER(S)	5. MONITORING ORGANIZATION REPORT NUMBER(S)
6a. NAME OF PERFORMING ORGANIZATION: Ballistic Research Laboratory; 6b. OFFICE SYMBOL (If applicable): ASCBR-IB-A	7a. NAME OF MONITORING ORGANIZATION
6c. ADDRESS (City, State, and ZIP Code): Aberdeen Proving Ground, MD 21005-5066	7b. ADDRESS (City, State, and ZIP Code)
8a. NAME OF FUNDING / SPONSORING ORGANIZATION; 8b. OFFICE SYMBOL (If applicable)	9 PROCUREMENT INSTRUMENT IDENTIFICATION NUMBER
8c. ADDRESS (City, State, and ZIP Code)	10. SOURCE OF FUNDING NUMBERS

PROGRAM ELEMENT NO	PROJECT NO	TASK NO	WORK UNIT ACCESSION NO
61102A	1L161102AH43	00	00

11. TITLE (Include Security Classification)
A Two-Phase Flow Simulation of LOVA Propellant Interior Ballistic Behavior Using the XNOVAK Code

12. PERSONAL AUTHOR(S)
George E. Keller and Albert W. Horst

13a. TYPE OF REPORT	13b. TIME COVERED	14 DATE OF REPORT (Year, Month, Day)	15 PAGE COUNT
Technical Report	FROM Jan 85 TO May 86		

16. SUPPLEMENTARY NOTATION

17. COSATI CODES			18. SUBJECT TERMS (Continue on reverse if necessary and identify by block number)
FIELD	GROUP	SUB-GROUP	
19	01		Gun Propellant, High Velocity, Guns
21	02		Interior Ballistics

19 ABSTRACT (Continue on reverse if necessary and identify by block number)

The interplay between igniter and propellant in high-performance gun systems has been the subject of many investigations, both theoretical and experimental, over the past decade. With the development of one-dimensional and two-dimensional, two-phase flow codes such as NOVA and TDNOVA, the propelling charge designer has become able to model mechanical aspects of the charge in increasing detail. Rational evaluation has been made possible of influences of ignition source location, the distribution of ullage, and the properties of packaging and other parasitic components.

However, the development of combustion submodels has lagged behind the treatment of hydrodynamic aspects of the interior ballistic cycle. In nearly all reported studies, the igniter has been modeled as a source of hot gas of

20 DISTRIBUTION / AVAILABILITY OF ABSTRACT	21 ABSTRACT SECURITY CLASSIFICATION	
☐ UNCLASSIFIED/UNLIMITED ☒ SAME AS RPT ☐ DTIC USERS	Unclassified	
22a NAME OF RESPONSIBLE INDIVIDUAL: George E. Keller	22b TELEPHONE (Include Area Code): (301)-278-6190	22c OFFICE SYMBOL: SLCBR-IB-A

DD FORM 1473, 84 MAR 83 APR edition may be used until exhausted
All other editions are obsolete

SECURITY CLASSIFICATION OF THIS PAGE
UNCLASSIFIED

continuation of 19. Abstract

predetermined flow rate, creating a convective stimulus to which the propellant responds as an inert substance until a predetermined surface temperature level is reached and steady-state combustion is assumed to commence. Yet, a great deal of success has been achieved despite these assumptions, while at the same time avoiding the complexity and cost of a more realistic treatment of ignition and combustion. Unfortunately, recent experience with low-vulnerability (LOVA) gun propellants has, on occasion, revealed large disparities between predictions and experimental performance.

In response to this problem, a new code known as XNOVAK has been developed to provide the capability of addressing a broad range of chemical reactions within the framework of a one-dimensional, macroscopic two-phase flow interior ballistic model. The new code allows for phase- and species-partitioning of the igniter output, an arbitrary number of reactions among the igniter and propellant product species, and subsurface heating due to chemical reactions. In this paper, the code is exercised using a data base for a 105-mm tank gun firing a LOVA-type propellant. While experimental data for many of these newly-available inputs are yet unavailable, the sensitivity of results to a limited range of values is investigated.

TABLE OF CONTENTS

LIST OF ILLUSTRATIONS

LIST OF TABLES

I. BACKGROUND

A. Recent Advances in Interior Ballistic Modeling

Over the past decade, the field of interior ballistic modeling has undergone a number of major advances. Early lumped-parameter models, which appeared in abundance as computer codes[1] in the mid-1960's, provide the charge designer with powerful tools to perform large, parametric interior ballistic studies rapidly and efficiently. These codes embody such assumptions as uniform and instantaneous ignition of the entire propellant charge, with combustion taking place in a uniformly varying, well-stirred mixture, the burning rate being determined by the instantaneous, "space-mean" gas pressure. A pressure gradient within the gun tube is typically superimposed on this solution to provide an appropriately reduced projectile base pressure, but these codes cannot address the physical hydrodynamics of the problem as manifested in ignition-induced pressure waves. Nonetheless, lumped-parameter codes have been and are still used throughout the world for most basic interior ballistics systems and charge design studies.

However, the prevalence of gun malfunctions, the origins of which were ultimately traced to ignition-related pressure waves[2,3] was sufficient motivation to launch an active new field -- that of multiphase flow interior ballistic modeling -- with participants from the government, academic, and industrial communities. First on the scene were one-dimensional, two-phase flow models[4-6], the primary purpose of which was to assess the influence of the ignition stimulus on flamespreading and the formation of pressure waves.

Probably the most successful and certainly the most used of these is the NOVA code[7], developed by Paul Gough Associates in response to pressure-wave problems experienced in Navy 5-inch guns. NOVA consists of a two-phase flow treatment of the gun interior ballistic cycle formulated under the assumption of quasi-one-dimensional flow. Functioning of the igniter is included by specifying a predetermined mass injection rate as a function of position and time. Flamespreading is driven by axial convection, the propellant responding as an inert substance until a predetermined surface temperature is reached. Propellant combustion then follows the same pressure-dependent description used in the lumped-parameter code -- this time, however, a locally prescribed rate dependent on the local instantaneous pressure. (Several other ignition and combustion options are available in some versions of the code but are largely untested.) In addition, internal boundaries defined by discontinuities in porosity are treated explicitly, and a lumped-parameter treatment is included to reflect the inertial and compactibility characteristics of any inert packaging elements present between the propellant bed and the base of the projectile. The literature includes numerous successful applications of this code to cased ammunition problems[8,9].

Next in the progression of modeling achievements were several quasi-two-dimensional treatments, in which coaxial regions of propellant and circumferential ullage are treated as coupled regions of one-dimensional flow. Thus, the influence of ullage external to a bagged

artillery charge on the path of flamespreading and the equilibration of pressure gradients can be estimated. Other aspects of the level of modeling are, however, in basic agreement with that of NOVA, including the simple surface temperature ignition criterion and the global, pressure-dependent combustion process assumed to occur at the propellant surface.

More recently, emphasis has been placed on fully two-dimensional interior ballistic models. TDNOVA[10-13] provides an axisymmetric description of macroscopic flow and includes many special features to model the fluid dynamics particular to stick propellants and rigidized combustible charges. A great deal of success modeling both granular and stick propellant artillery charges has been achieved with this code[14,15]. The emphasis to date, however, continues to be in regard to increasing the fidelity of the treatment of the configural complexities of the propelling charge and gun chamber rather than that of the detailed ignition and combustion processes themselves, and the same simple models for ignition and combustion as described above continue to be used in most studies. Yet, such codes as NOVA and TDNOVA have provided today's charge designer with the capability to evaluate computationally the influences of the location of the ignition source, distribution of ullage, and mechanical characteristics of containers or other parasitic elements in which the propellant is packaged.

B. The Case for Improved Reaction Kinetics

The emphasis on hydrodynamics has resulted not from a lack of interest in the ignition and combustion processes themselves but rather from a belief that no real progress could be made in modeling flamespreading and pressure-wave phenomena in many real-world charges until an overall modeling framework was established which recognized the associated configural complexities of the problem. With TDNOVA representing a major step toward providing this capability, we now must seriously face the next level of deficiencies appearing to impede further progress. Ample direct and indirect evidence exists to suggest that the shortcomings of our ignition and combustion submodels can no longer be overlooked.

Very long ignition delays (tens to hundreds of milliseconds) often accompany the low-pressure ignition event encountered with artillery charges; however, measured heat input to the propellant suggests that the propellant should reach its ignition temperature in just a few milliseconds. Further, high-speed movies of ignition and flamespreading in transparent howitzer simulators show first luminosity (following that of the igniter itself) often to be in the gas-phase regions of ullage downstream from the propellant bed; first propellant combustion with visible flame within the bed itself is also often considerably downstream of the ignition source.

The presence of some significant gas-phase chemistry is also suggested by the occasional, vigorous combustion event (e.g., breechblow) which accompanies extremely long ignition delays exhibited in firings of cold-conditioned charges. Indeed, the widely observed phenomenon of increasing chamber pressures with increasing levels of pressure waves requires either propellant grain fracture or some form of

transient burning rate enhancement (or both) for its explanation.

Somewhat more subtle but still of extreme importance to the gun community has been recent experience with low-vulnerability (LOVA) gun propellants, which has revealed, on occasion, large disparities between calculated and experimental performance. A recent study of ballistic anomalies exhibited by one lot of experimental LOVA propellant highlighted the possible interplay between flamespreading rates and ballistic performance for hard-to-ignite propellants[16]. However, the combustion mechanism for such compositions, particularly at low pressures, may in no way resemble a simple, global reaction at the propellant surface. Early binder decomposition yielding fuel-rich products may yield likely candidates for subsequent gas-phase reactions, with potentially significant influence on the ensuing flamespreading process.

LOVA test firing results, furnished by S. E. Mitchell[17], are shown in Table 1. The system under study was a 105-mm tank gun. An M490 TP-T Cartridge was fitted with a modified M489 Projectile, with the projectile weight chosen to simulate an M456A2 HEAT-T-MP round. The firings summarized were all performed at 294K, nominal ambient temperature. Important differences were observed as a function of the igniter material alone; some characteristics of the igniters are shown in Table 2. Note that the igniters labeled "R" and "Z" are rich in available oxygen. Certainly one interpretation of these results is that the igniter material participates chemically in the combustion, as well as ignition, of the solid LOVA propellant. The studies reported in this paper were performed with just that idea in mind.

Table 1. Performance Variations As a Function of Igniter Material

Igniter Name	Peak Pressure (MPa)	Muzzle Velocity (m/s)
Benite	307	1078
"R"	368	1141
"Z"	426	1191

Table 2. Igniters

Igniter Name	Flame Temperature (K)	Impetus (J/g)	Oxygen Mole Fraction of Total Gas at Equilibrium (%)
Benite	2518	561.3	0
"R"	3251	604.9	22
"Z"	3541	730.4	13

C. Framework for Study

To investigate the potential influences of a broad range of chemical interactions on flamespreading and subsequent interior ballistic processes, an extremely rugged and computationally efficient version of the NOVA code, known as XNOVA, was further modified by Paul Gough Associates to include a number of revisions to the ignition and combustion submodels[18,19].

The ignition model has been extended to treat igniters whose products of combustion are multiphase. The combustion products are treated as a reacting homogeneous mixture composed of an arbitrary number (presently, as many as ten) of chemical species, each of which is either a gas or an aggregate of finely divided droplets or particles. An arbitrary number of chemical reactions (again, as many as ten) is admitted among the species. The influence of deposition of the condensed species onto the surface of the solid propellant is considered both in respect to the changing composition of the flowing mixture of combustion products and the thermal response of the propellant. The mass transferred to the mixture as a result of local decomposition of the propellant is not assumed to consist of final products of combustion. The transferred material may be described as intermediate products of combustion which release the full energy of combustion only after further chemical reaction in the mixture. Chemical interactions between the igniter combustion products and the intermediate products of the propellant may therefore be modeled. The analysis of the thermal response of the propellant includes the contributions of subsurface heating due to chemical reaction. The boundary conditions at the heated surface include an energy balance which reflects both the external ignition stimulus and the heat feedback from the near-field flame, and either a pyrolytic or an evaporative condition to determine the surface regression.

In this report, we first probe the operational status of several of the more interesting options with respect to a nominal data base for a 105-mm tank gun firing a LOVA propellant. We then address application of the integrated capabilities of the extended code, XNOVAK, to a class of real-world ballistic problems appropriate to the selected problem. Finally, we will draw some conclusions about the most fruitful directions for further study, both theoretical and experimental, in this area.

II. AN EXAMINATION OF NEW MODELING FEATURES OF XNOVAK

A. Input Data

For these studies, we chose to model a 105-mm, M68 Tank Gun, firing the M456A2 HEAT-T-MP cartridge loaded with LOVA propellant. Since XNOVAK provides a one-dimensional (with area change) representation of flow, some compromise in configural aspects of the problem was required, as depicted in Figure 1.

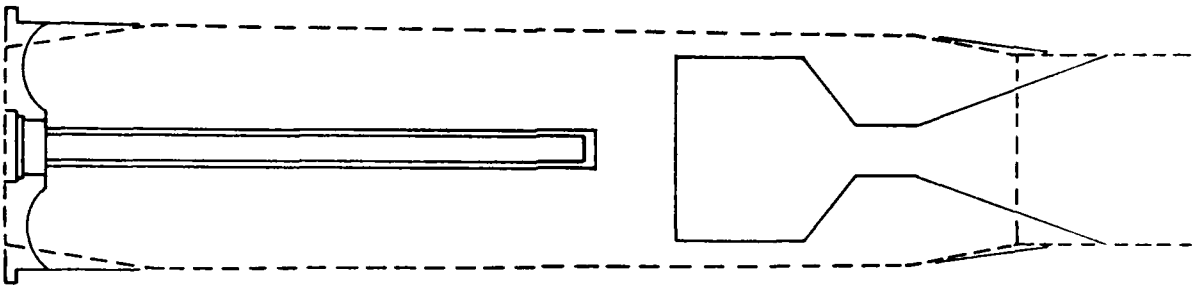

Figure 1. Representation of the Problem

The baseline XNOVAK calculation for the 105-mm, M68 Tank Gun firing the M456A2 Cartridge loaded with 6.056 kg of LOVA propellant (XM39, Lot A2-202) employed the input data shown in Table 3. In addition to the usual propellant data, we used rheology data appropriate to NACO propellant, in the absence of better data. The rheology data were varied from time to time, during the course of the study, to ensure that the results of the study were not unduly influenced by this choice of data.

Table 3. Propellant Input Data

Propellant Type:	LOVA XM39 Lot A2-202
Mass of Propellant (kg):	6.056
Density of Propellant (g/cm^3):	1.619
Outside Diameter (mm):	7.772
Perforation Diameter (mm):	0.381
Length (mm):	8.636
Number of Perforations:	19
Speed of Compression Wave in Settled Bed (m/s):	442.
Speed of Expansion Wave (m/s):	1270.
Ignition Temperature (K):	477.
Chemical Energy Released in Burning (J/g):	3897.
Molecular Weight:	20.954
Ratio of Specific Heats:	1.2812
Covolume (cm^3/g):	1.028

Available propellant burning rate data for the subject propellant are shown in Figure 2. The strand burner probably provides a more reliable source of low-pressure burning rate data, eliminating the ambiguity in closed bomb results in this region, where ignition and flamespreading may be influencing results. The burning rates used in the simulations are shown in Table 4, along with the values for B and n, for the customary burning rate law, Bp^n, that are deduced from them.

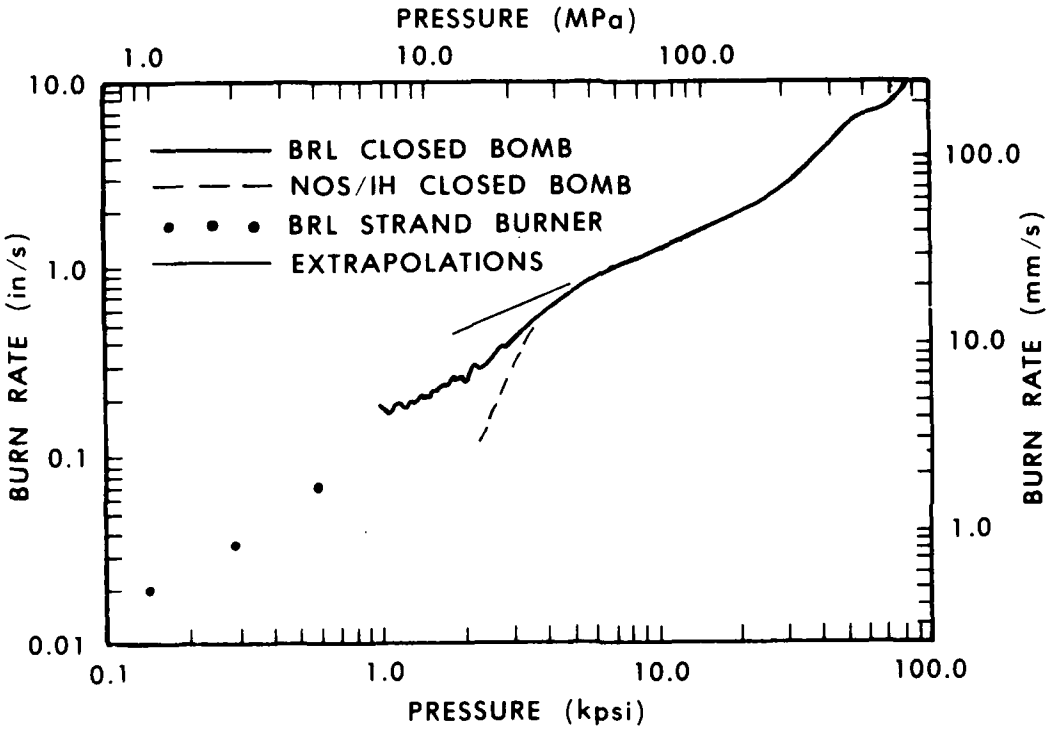

Figure 2. Burning Rates, LOVA XM39 Lot A2-202

Table 4. Propellant Burn Rates

Pressure (MPa)	Burn Rate (mm/s)
2.0	0.883
41.38	25.4
137.9	50.8
551.7	254.0

Table 4. Propellant Burn Rates (continued)

$$Rate = B * P^{n}$$

Upper Pressure Bound (MPa)	B (mm/(s-(MPa)^{n}))	n
41.38	0.409438	1.1088
137.9	2.977376	0.5758
551.7	0.166814	1.1608

XNOVAK, like its predecessor, models the igniter function as a deposition of mass as a function of position and time. The igniter is assumed to function for four milliseconds, with maximum output from its rear outlet holes and minimum output from its front outlet holes. This function is depicted graphically as Figure 3.

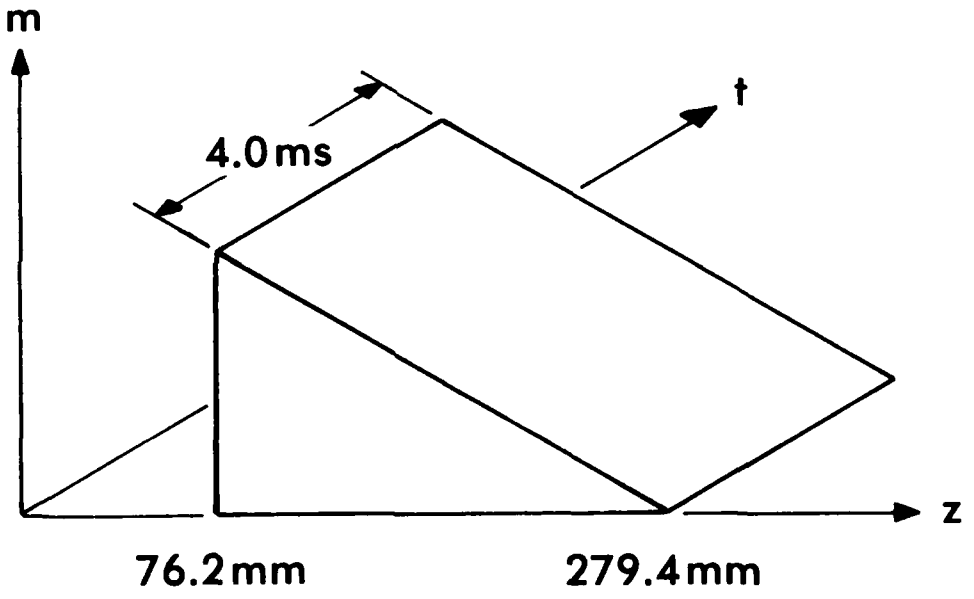

Figure 3. Igniter Output

B. Sensitivity to Burning Rates

Since many of the new features of XNOVAK are in response to a perceived need to provide a more accurate representation of the rate of energy release from propellant combustion, particularly at low pressures, we felt it important to test this premise in terms of the sensitivity of calculated results to the low-pressure burning rates described above. In the absence of good, low-pressure burning rate data, provided in this case by the BRL strand burner, one might have chosen to describe the process by just two straight-line segments, attributing the data fall-off at pressures less than 40 MPa to flamespreading. Given the definitive low-pressure data, however, a

third burning rate slope is defined which fixes burning rates at low pressures at values much lower than the "two-slope" description.

The ballistic consequences of this difference are shown in Table 5. The maximum pressure and the muzzle velocity for the "two-slope" case reflect the fact that, with higher burning rates at low pressures, propagation of flame through the main charge, as well as combustion of propellant behind the flame front, advance much more rapidly, and at completion of flamespreading, the pressure, velocity, and acceleration are all greater than for the "three-slope" case. Indeed, the calculated performance (and, presumably, actual gun performance as well) reveals a strong dependence on the rate of energy release early in the interior ballistic cycle. Naturally, the remaining studies reported in this paper all employed the "three-slope" burning rate description. In the Appendix, BASE3 is the resulting input data file which forms the foundational data base for the work reported here.

Table 5. Influence of Low-Pressure Burning Rate Data

	Peak Pressure (MPa)	Muzzle Velocity (m/s)
2 slopes	523	1267
3 slopes	448	1235

C. Sensitivity to Igniter Output

As before, the output of the igniter in XNOVAK is described in terms of a mass flux as a function of axial position and time. Now, however, it can be apportioned between the gas, liquid, and solid phases as well , though the distinction between the liquid and solid condensed phases is purely formal at this time. A major difference in the treatment of the gas and condensed phases is that the condensed phases may be deposited on the surface of the propellant surface, significantly enhancing heat transfer to the solid propellant, while altering the mixture of igniter combustion products in the flow. In the code, mass transfer from the condensed phases of the igniter output to the solid propellant is described by equation 1,

$$\dot{w}_i = k_i Y_i \rho (u-u_p)^2 (1-\varepsilon), \quad , \quad (1)$$

in which the rate of mass transfer is proportional to the concentration of the solid propellant and the relative momentum flux of the mixture of combustion products. Here k_i is an empirical coefficient that should depend on the diameter of the individual particles or droplets which constitute the condensed species and ε is the porosity of the two-phase mixture. The condensed products of the igniter are assumed to be sufficiently finely divided that they are deposited on the surface of the solid propellant as a uniform layer, so that there are no "hot spots." At deposition, the mass and heat of the condensed species is transferred to the solid propellant, the temperature of the condensed species is instantaneously equilibrated with the (increased) surface

temperature of the solid propellant, and the mass and heat of the condensed species are lost to the mixture of combustion products.

Table 6 illustrates the results obtained upon varying the transfer coefficient, k_i, and the ratio of gas to condensed igniter products, the former from 0.0 to 0.00001 and the latter from 1.0/0.0 (all gas) to 0.1/0.9 (one part gas to nine parts condensed). The value 0.00001 was chosen arbitrarily. (For these tests, there were assumed to be no chemical reactions among igniter products and propellant gas-phase species, and there were no intermediate propellant species. All the energy contained in the solid propellant was liberated at the instant of burning, which was described by the customary Bp^n burning rate law.) In the Appendix, BASE5 is the input data base that was used.

Consider first the top three rows of Table 6. Row one represents our baseline calculation, with the igniter producing gaseous products only. When the igniter output is split 50/50 in the second calculation, we see that the gun performance is degraded. Close examination of the results of the simulation reveals that with diminished igniter output (after all, the condensed phase is contributing nothing to the heating of the solid propellant, the transfer coefficient being zero), at the completion of flamespreading, overall gas production has been less and the projectile velocity and acceleration are lower than for the baseline case. Ultimately, ballistic performance is reduced as well. In the third case, with just 10% of the igniter output serving to heat the propellant grains, the propellant surface temperature is never elevated sufficiently to achieve ignition. These results are not surprising and similar performance should be expected for any propellant.

Table 6. Effects of Transfer Coefficients and Gas/Condensed Igniter Output on Ballistics

Transfer Coefficient	Gas/ Condensed	Maximum Pressure (MPa)	Muzzle Velocity (m/s)	Time to 25.4 mm Travel (ms)
0.0	1.0/0.0	453	1238	2.9
0.0	0.5/0.5	445	1232	3.9
0.0	0.1/0.9	propellant did not ignite		
0.00001	1.0/0.0	453	1238	2.9
0.00001	0.5/0.5	451	1236	3.2
0.00001	0.1/0.9	439	1227	4.5

The second set of three calculations is more interesting. The first of the three (the calculation represented by the fourth row) is our baseline again, repeated for clarity; the igniter output is all gas, so the fact that the transfer coefficient is not zero is immaterial. In the second case (the fifth row), the condensed species do contribute to the heating of the solid propellant, and gun performance is improved from the calculation shown in row 2, nearly enough to restore baseline levels (with the chosen value of the transfer coefficient, k_i). The final calculation is the most interesting of all. The gas pressure is low, flamespreading is slow, and the apparent "ignition delay" increases still more, as indicated by the increase in

the time to projectile motion. Ballistic performance is marginally, but measurably, less than in previous cases.

Figure 4, simultaneously depicting flamespreading and projectile motion for the second set of three calculations, was constructed to provide some insight into these results. On the left are plotted the paths of flame propagation, emanating both forward and rearward from the axial region over which primer venting is prescribed to have taken place. To the right are plotted the corresponding projectiles' inbore trajectories, each terminating in this figure at its time/position of maximum chamber pressure. The interplay between flamespreading and early projectile motion is of particular interest, since the projectile has been observed to start to move before flamespreading is complete when LOVA-type propellants are in use. Such behavior is potentially beneficial in terms of its influence on overall performance level but is believed to impact unfavorably on performance reproducibility.

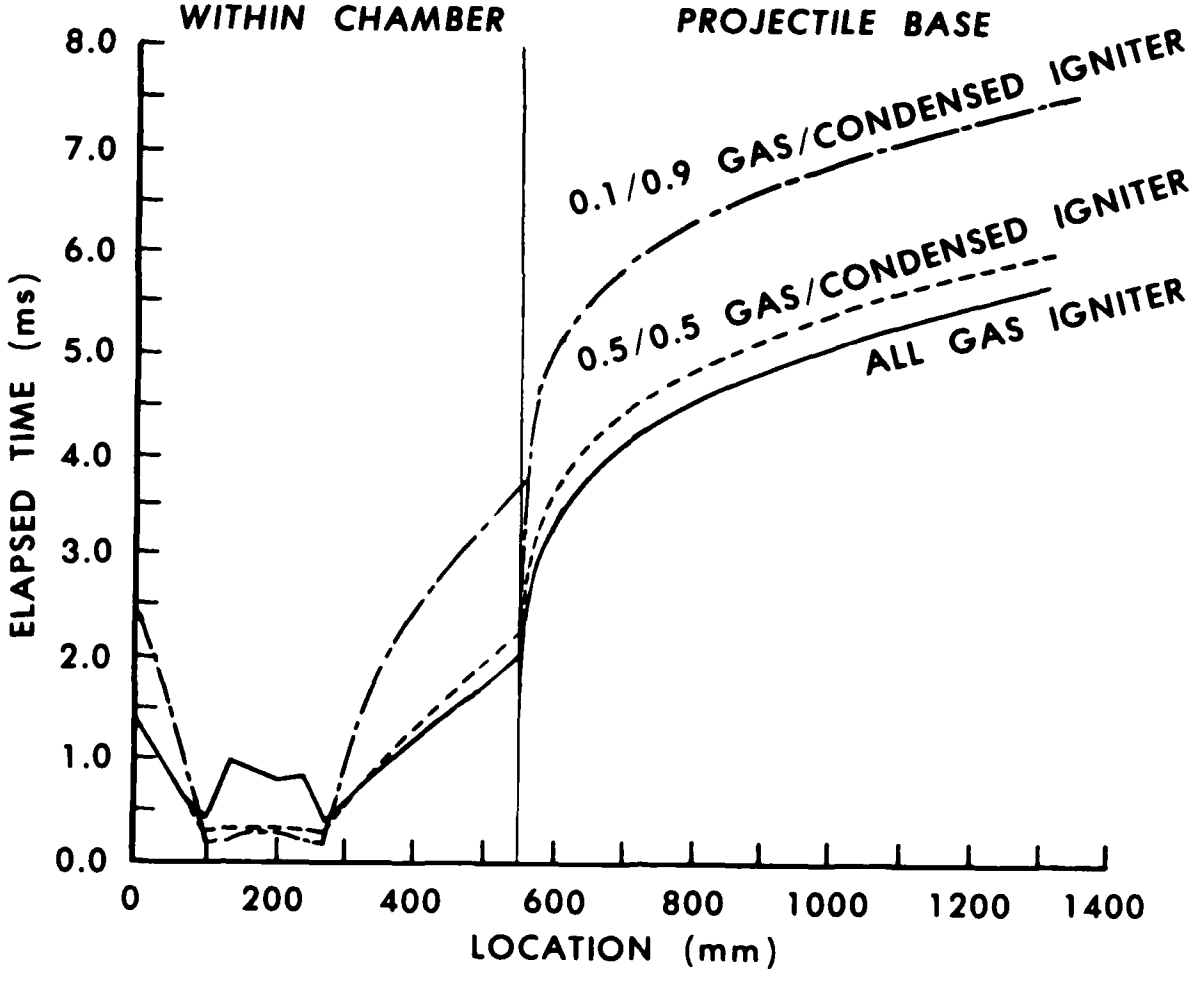

Figure 4. Flamespreading and Projectile Motion

The solid curve in Figure 4 represents our baseline calculation. The propellant ignites most quickly at the ends of the igniter (convection being greatest at the two ends of the region of primer venting -- a consequence of the one-dimensional representation), rapidly driving flamespreading to completion in about 2 ms. Projectile motion begins just before flamespreading is complete.

The dashed curve in Figure 4 corresponds to the calculation summarized in the fifth row of Table 6; the igniter output is split equally between gas and condensed-phase species. The convective stimulus is now augmented by the efficient heating associated with deposition of the condensed-phase products on the propellant surfaces and results in very rapid ignition in the region of primer venting. Gas pressure resulting from igniter products, however, is less, reducing the convective stimulus to the extreme ends of the main propellant charge and delaying completion of flamespreading. At the time flamespreading is complete, the projectile has moved somewhat farther down the bore, resulting in more available free volume for the corresponding fraction of propellant burned. The ultimate result is a lower peak pressure at a greater projectile travel, with an accompanying lower projectile muzzle velocity.

The dot-dashed curve in Figure 4 depicts the results from the calculation for which 90% of the igniter output was condensed and only 10% was gaseous. While the propellant adjacent to the igniter is seen to ignite very rapidly, the low level of igniter gas production leads to a correspondingly low level of pressurization, so that convectively driven flamespreading into regions remote from the primer is even slower than in the previous case. As a result, the free volume is even greater at the completion of flamespreading, and the ballistics suffer accordingly.

While the specific results obtained from this series of calculations are believed to be highly dependent on the interplay among a number of input values of questionable validity (e.g., igniter output characteristics, propellant ignition temperature, and engraving pressure profile), the important result here is that the resulting variation in predicted performance confirms the potential ballistic consequence of such mechanisms as these.

D. Gas-Phase Reactions

The present extension incorporated in XNOVAK recognizes the possibility of chemical reactions occurring in the mixture of combustion products. As outlined above, an arbitrary number of reactions is admitted, involving an arbitrary number of chemical species. All reactions are assumed to have rates governed by a general Arrhenius law. We also model reactions in which a group of reactants may interact with a spectator molecule which is itself unchanged by the reaction. Each reaction is assumed to proceed in the forward direction only:

$$\sum_{i=0}^{n} \nu'_{ik} S_i \rightarrow \sum_{i=0}^{n} \nu''_{ik} S_i , \qquad (2)$$

where S_i is species i and ν_{ik}' and ν_{ik}'' are the stoichiometric coefficients for reactants and products respectively. We extend the summation to include i=0, which is understood to incorporate formally a reaction in which a spectator molecule may participate.

The rate of reaction k is r_k, where

$$\dot{r}_k = B_k T^{\beta_k} \exp\left[-\frac{E_k}{R_u T}\right] \prod_{i=o}^{N} (Y_i \rho)^{\nu_{ik}'''} \quad . \qquad (3)$$

We note that the reaction order of ν_{ik}''' may differ from that of ν_{ik}', since for many applications of interest, reaction k will be a global rather than an elementary reaction. The rate of production of species i by reaction k is

$$\dot{r}_{ik} = (\nu_{ik}'' - \nu_{ik}')\dot{r}_k , \qquad (4)$$

per unit volume of the mixture.

Since it is expected that the code will be applied to situations in which the reactions are of the overall or global type rather than the fundamental type, we have assumed that the chemical rates will have time constants which are comparable to times of ballistic interest. Accordingly, there is no provision for chemical schemes in which certain of the reactions are very short in comparison with the others. If interest is eventually directed towards more fundamental schemes, it will be necessary to incorporate a stiff integration package to handle the chemical reactions in the balance equations.

We continue the present study according to the following scenario. For simplicity, the igniter is assumed to release all of its output in the gas phase. The gaseous products convectively heat the surface of the solid propellant, which reaches the prescribed ignition temperature and begins to regress at a rate defined by Bp^n. During regression, it is assumed that half of the total chemical energy available during complete combustion of the propellant is released; the other half is available to be released during subsequent (flame-zone) reactions. This choice of half of the energy being released at or near the surface and half being released in the flame zone, is guided by the work of Zenin[20]. Again for simplicity, the regression is assumed to produce a gaseous species which we call LOVA-I, an "intermediate state" associated with combustion of the subject LOVA propellant. When LOVA-I further reacts, LOVA-F, a final gaseous state of LOVA is formed, and the other half of the energy of the solid propellant is released. Naturally, these proportions can be adjusted, but we have few data for guidance at this time. In the Appendix, BASE6 is the input data file that was used.

The results summarized in Table 7 characterize the rate dependence of predicted ballistic results, assuming that the reaction of LOVA-I to LOVA-F takes place (at a rate defined by an activation energy of 7.5 x 10^4 Joules/mole and a pre-exponential factor as shown in the table) due to collisions with any gaseous species, here represented by the

traditional "M." The values of activation energy and of pre-exponential factor were guided by the suggestions of Price[21], which are based on work at the Naval Weapons Center, China Lake, CA[22-27]. In this case, there are four gaseous species: air, igniter gas, LOVA-I, and LOVA-F; a collision with any one of them has the same potential for reaction. Table 7 thus defines the range of the pre-exponential factor necessary to transition from the condition in which few of the LOVA-I's have reacted to form LOVA-F's to the condition in which essentially all have reacted. For the latter case, the performance of our initial baseline calculation, described earlier in the paper, is regained. For the former, nearly a quarter of the available propellant energy is wasted, blown out the muzzle unused, so that the gun performance falls off markedly. As the reaction rate coefficient of the single reaction increases, not only is a larger fraction of the LOVA-I converted to LOVA-F, but also the conversion takes place earlier in time. Thus, Table 7 also shows that ballistic performance improves as the propellant energy is released earlier in the ballistic cycle. Interestingly, the apparent "ignition delays" for this wide range of rate coefficients are essentially identical, presumably because the projectile started moving before there was any appreciable "flame-zone" reaction.

Table 7. One Gas-Phase Reaction

LOVA-I + M -> LOVA-F + M

B = pre-exponential factor
E = activation energy = 7.5E4 Joules/mole

B (cm^3/g-s)	Peak Pressure (MPa)	Muzzle Velocity (m/s)	LOVA-F/LOVA-total at muzzle
5.42E5	151	785	0.522
7.23E5	217	992	0.927
9.03E5	292	1096	0.962
1.08E6	337	1144	0.976
2.17E6	429	1220	0.994
3.61E6	444	1230	0.996

Figure 5 depicts graphically the evolution of mass fractions of intermediate and final products for the slowest reaction shown in Table 7. The air in the gun tube at the start of the cycle quickly diminishes as a fraction of the total gas present, since there is no source for more air. The gaseous output of the igniter builds up early in the cycle but then diminishes as LOVA gas is produced. LOVA-I, the intermediate gaseous state of the burning solid propellant, is produced as soon as the igniter heats the solid propellant to the prescribed ignition temperature. Half of the energy of the solid propellant is released when LOVA-I is produced. Collisions of LOVA-I with any of the other species lead to reactions that form LOVA-F, liberating the remainder of the solid-propellant energy.

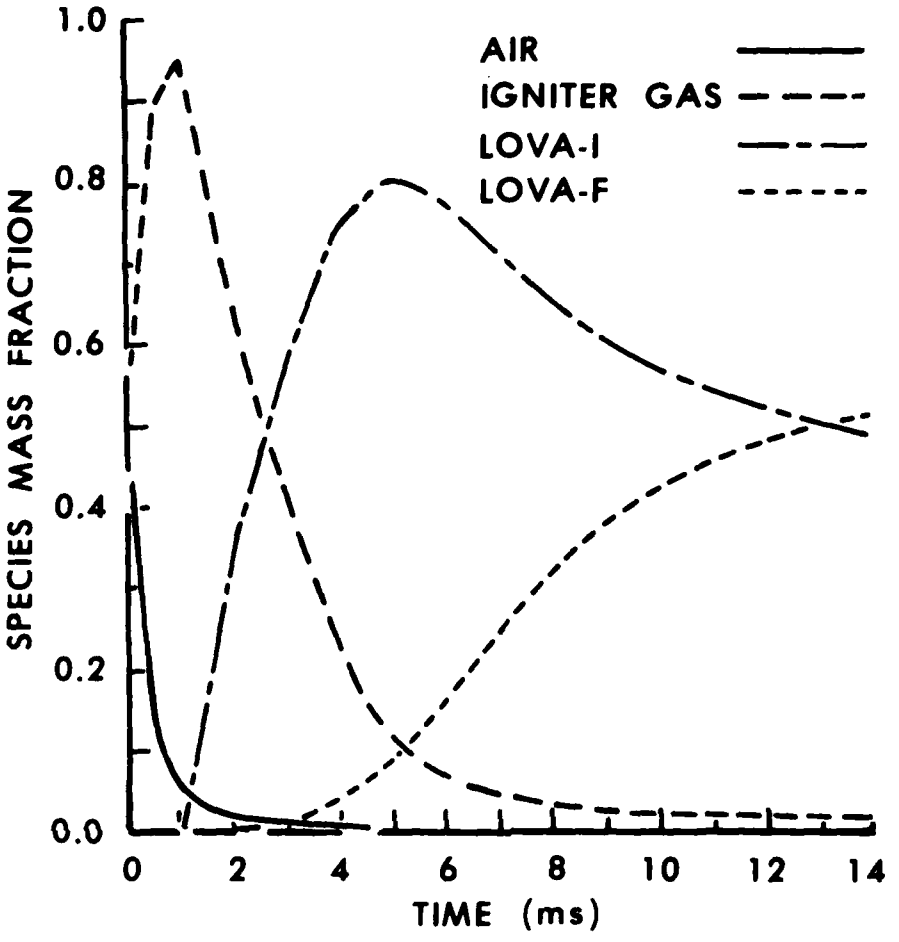

Figure 5. Evolution of Mass Fractions for One Gas-Phase Reaction

The real significance of these results is that since the several assumed parameters of this simulation should be at least approximately correct these calculations should then define a critical value for the reaction rate of the flame zone reaction. If, indeed, overall effective rates of the two or more steps in the combustion of LOVA propellant were in this range, erratic performance of the gun would likely result, and certainly experimental gun performance could not be adequately simulated by the use of standard lumped-parameter codes.

In Table 8, we attempt to depict the impact of adding just one more reaction, a chemical reaction between the LOVA-I's and the igniter gases, to the above scheme. This second reaction is assumed to have the same activation energy as the first and to take place with a rate which varies in accordance with the pre-exponential factor. The series of calculations summarized in Table 8 identifies the range of rates over which this additive reaction "restores" the performance of the gun by hastening the conversion of LOVA-I to LOVA-F, with the concomitant

liberation of energy. No claim is made that this is the "right" reaction to have added; this is simply a second reaction that comes to mind - especially a mind motivated by the test firings mentioned above. This second additive gaseous reaction permits the igniter to participate in a second, important fashion; after heating the solid propellant grains, its output gases are available to enter into or influence subsequent chemical reactions in the flame zone. While the addition of this particular second reaction does not fully restore the performance of the gun to that of the baseline case, this second reaction path does markedly increase the the fraction of LOVA-I that is transformed to LOVA-F, improving performance accordingly. In the Appendix, BASE7 is the data file that was used. An echo of the BASE7 input by XNOVAK is also included in the Appendix.

Table 8. Two Gas-Phase Reactions

(1) LOVA-I + M -> LOVA-F + M

E(1) = 7.5E4 Joules/mole
B(1) = 3.25E5 $cm^3/g-s$

(2) LOVA-I + Igniter(G) -> LOVA-F + Air

E(2) = 7.5E4 Joules/mole

B(2) ($cm^3/g-s$)	Peak Pressure (MPa)	Muzzle Velocity (m/s)	LOVA-F/LOVA-total at muzzle
3.61E5	155	801	0.593
1.08E6	161	826	0.675
3.61E6	176	872	0.763
1.08E7	190	909	0.806
3.61E7	200	931	0.826
1.08E8	206	943	0.835

The influence of this second reaction on the evolution of the gaseous species is shown in Figure 6, using the data corresponding to the fastest second reaction of Table 8. The igniter gas still peaks early, but then is reduced both by its limited quantity and by the early influence of the second gas reaction. The mass fraction of air drops early but peaks again as air is formed in accordance with the postulated second reaction. LOVA-I is depleted by both reactions, and its mass fraction is lower at the end of the ballistic cycle than for the single reaction case; LOVA-F is created by both reactions, and its final mass fraction is higher.

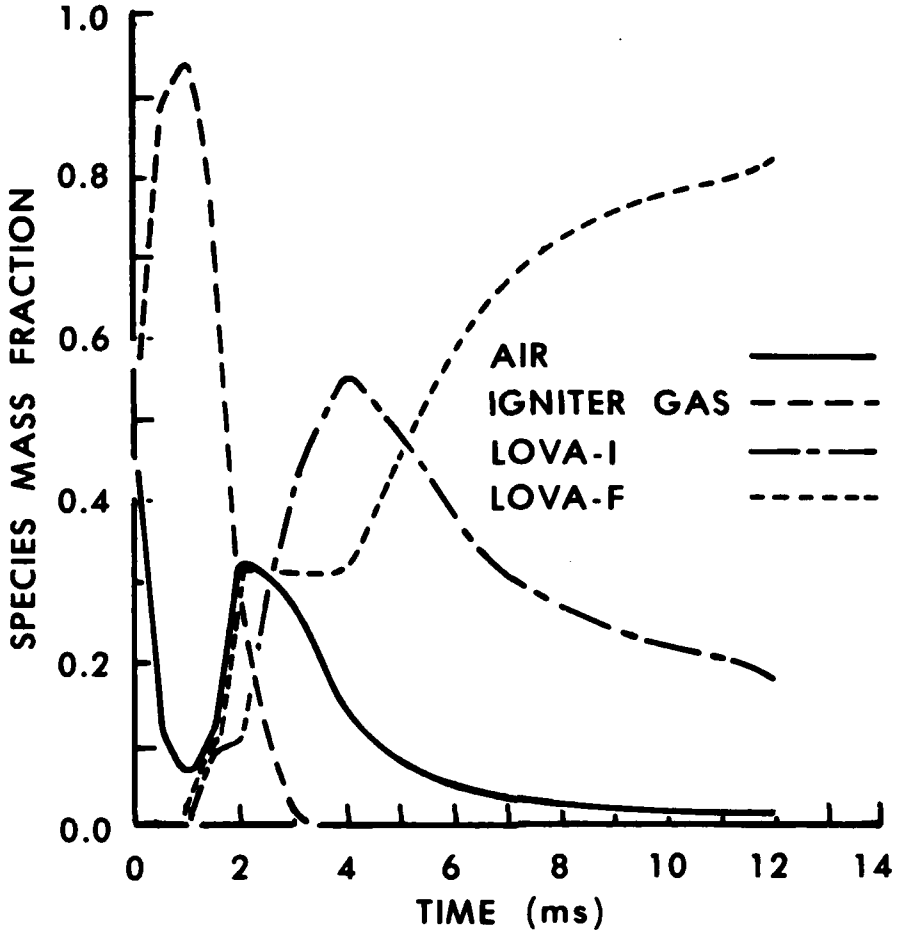

Figure 6. Evolution of Mass Fractions for Two Gas-Phase Reactions

IV. CONCLUSIONS

While the vast majority of past problems plaguing the gun propelling charge designer have been successfully addressed without any real description of reaction kinetics, the more stringent ignition requirements posed by some of the newer propellants specifically developed to exhibit low-vulnerability characteristics have brought about the need for more advanced modeling capabilities. The XNOVAK code has shown itself to be both rugged and versatile in this application, allowing the investigator to examine the effectiveness of igniters both insofar as initiating combustion of the solid propellant and also in terms of influencing any subsequent reactions taking place within the mixture of combustion products. Given a few data in respect to these reactions, the code should be useful in identifying the ranges over which other parameters become important. At this point, however, the practicality of results has been limited by the sparsity of such information. Here at the BRL, the efforts of Miller et al.[28-32] are directed toward the production of data which are directly applicable to codes like XNOVAK, so that the future holds promise.

The interior ballistic and the combustion communities must continue to cooperate in identifying mechanisms and providing descriptions of reactions on a level appropriate for inclusion into state-of-the-art interior ballistic codes. A full appreciation for each other's capabilities and problems is only now being developed, but cooperative efforts have begun to define appropriate experimental techniques for specifying and quantifying important gun-environment reactions of potential ballistic consequence. Ultimately, such information, used in codes like XNOVAK, will allow the charge designer to specify the optimal chemical composition as well as spatial and temporal characteristics for matching ignition systems to new propellants and charge configurations.

ACKNOWLEDGMENTS

Without the efforts of Paul Gough, over many years, this work would not have been possible. We acknowledge the assistance of Steve Mitchell, whose cooperation in providing test firing results put this work into proper perspective. Thanks are due to Chan Price and his colleagues at China Lake for their encouragement of this project. Finally, we thank Martin Miller for his effort in producing the strand burner data, for his efforts to produce data for use in codes like XNOVAK, and for his excellent review of this manuscript.

REFERENCES

1. P. G. Baer and J. M. Frankle, "The Simulation of Interior Ballistic Performance of Guns by Digital Computer Program," BRL Report No. 1183, USA ARDC, Ballistic Research Laboratories, Aberdeen Proving Ground, MD, December 1962.

2. A. J. Budka and J. D. Knapton, "Pressure Wave Generation in Gun Systems: A Survey," BRL MR 2567, USA Ballistic Research Laboratories, Aberdeen Proving Ground, MD, December 1975.

3. I. W. May and A. W. Horst, "Charge Design Considerations and Their Effect on Pressure Waves in Guns," ARBRL-TR-02277, USA ARRADCOM, Ballistic Research Laboratory, Aberdeen Proving Ground, MD, December 1980.

4. E. B. Fisher, "Continued Development and Documentation of the Calspan Interior Ballistics Code," Calspan Report No. 6689-D-1, Calspan Corporation, Buffalo, NY, February 1981.

5. P. S. Gough, The Flow of a Compressible Gas Through an Aggregate of Mobile Reacting Particles," IHCR 80-7, Naval Ordnance Station, Indian Head, MD, December 1980.

6. K. K. Kuo and J. H. Koo, "Transient Combustion in Granular Propellant Beds. Part 1: Theoretical Modeling and Numerical Solution of Transient Combustion Processes in Mobile Granular Propellant Beds," BRL-CR-346, USA ARRADCOM, Ballistic Research Laboratory, Aberdeen Proving Ground, MD, August 1977.

7. P. S. Gough, "The NOVA Code: A User's Manual. Volume 1. Description and Use," IHCR 80-8, Naval Ordnance Station, Indian Head, MD, December 1980.

8. A. W. Horst, T. C. Smith, and S. E. Mitchell, "Key Design Parameters in Controlling Gun-Environment Pressure-Wave Phenomena - Theory Versus Experiment," 13th JANNAF Combustion Meeting, CPIA Publication 273, Vol. 1, pp. 341-368, December 1975.

9. A. W. Horst and P. S. Gough, "Influence of Propellant Packaging on Performance of Navy Case Gun Ammunition," Journal of Ballistics, Vol. 1, No. 3, pp. 229-258, 1977.

10. P. S. Gough, "A Two-Dimensional Model of the Interior Ballistics of Bagged Artillery Charges," ARBRL-CR-00452, USA ARRADCOM, Ballistic Research Laboratory, Aberdeen Proving Ground, MD, April 1981.

11. P. S. Gough, "Two-Dimensional, Two-Phase Modeling of Multi-Increment Bagged Artillery Charges," ARBRL-CR-00503, USA ARRADCOM, Ballistic Research Laboratory, Aberdeen Proving Ground, MD, February 1983.

12. P. S. Gough, "Modeling of Rigidized Gun Propelling Charges," ARBRL-CR-00518, USA ARRADCOM, Ballistic Research Laboratory, Aberdeen Proving Ground, MD, November 1983.

13. P. S. Gough, "Numerical Simulation of Current Artillery Charges Using the TDNOVA Code," PGA-TR-85-1, Paul Gough Associates, Inc., Portsmouth, NH, March 1985.

14. A. W. Horst, F. W. Robbins, and P. S. Gough, "A Two-Dimensional, Two-Phase Flow Simulation of Ignition, Flamespread, and Pressure-Wave Phenomena in the 155-mm Howitzer," ARBRL-TR-02414, USA ARRADCOM, Ballistic Research Laboratory, Aberdeen Proving Ground, MD, July 1982.

15. A. W. Horst, F. W. Robbins, and P. S. Gough, "Multidimensional, Multiphase Flow Analysis of Flamespreading in a Stick Propellant Charge," ARBRL-MR-03372, USA ARRADCOM, Ballistic Research Laboratory, Aberdeen Proving Ground, MD, August 1984.

16. A. W. Horst, "Multiphase Flow Analysis of the Ballistic Performance of an Anomalous LOVA Propellant Mix," ARBRL-MR-03277, USA ARRADCOM, Ballistic Research Laboratory, Aberdeen Proving Ground, MD, June 1983.

17. Mitchell, S. E., personal communication.

18. P. S. Gough, "Theoretical Modeling of Navy Propelling Charges, PGA-TR-84-1, Paul Gough Associates, Inc., Portsmouth, NH, November 1984.

19. P. S. Gough, "Modeling Chemical Interactions in Ignition of Gun Propellant," Proceedings of the 22nd JANNAF Combustion Combustion Meeting, CPIA Publication 432, Vol I, pp. 223-237, October 1985.

20. A. A. Zenin, "Structure of Temperature Distribution in Steady-State Burning of a Ballistite Powder," Fizika Goreniya i Vzryva, Vol. 2, No. 3, pp. 67-76, 1966.

21. C. F. Price, personal communication.

22. M. W. Beckstead, N. L. Peterson, D. T. Pilcher, B. D. Hopkins, and H. Krier, "Convective Combustion Modeling Applied to Deflagration-to-Detonation Transition of HMX," Combustion and Flame, Vol. 30, pp. 231-241, 1977.

23. T. L. Boggs, C. F. Price, A. I. Atwood, D. E. Zurn, and R. L. Derr, "Role of Gas Phase Reactions in Deflagration-to-Detonation Transition," Seventh Symposium (International) on Detonation, Naval Surface Weapons Center, NSWC MP-82-334, pp. 216-224, June 1981.

24. C. F. Price, T. L. Boggs, J. L. Eisel, A. I. Atwood, and D. E. Zurn, "Gas Phase Kinetics During Normal Combustion," Proceedings of the 17th JANNAF Combustion Meeting, CPIA Publication 329, pp. 401-412, November 1980.

25. T. L. Boggs, C. F. Price, and R. L. Derr, "Transient Combustion: An Important Consideration in Deflagration-to-Detonation Transition," North Atlantic Treaty Organization Advisory Group for Aerospace Research & Development, Neuilly sur Seine, France, AGARD-CCP-367, pp. 12-1 to 12-20, May 1984.

26. C. F. Price and T. L. Boggs, "Modeling the Deflagration-to-Detonation in Porous Beds of Propellant," Eighth Symposium (International) on Detonation, Vol II, pp. 650-657, July 1985.

27. C. F. Price and T. L. Boggs, "A Simultaneous Mathematical Treatment of Deflagration and Ignition Phenomena," Proceedings of the 22nd JANNAF Combustion Meeting, CPIA Pub. 432, Vol I, pp. 505-513, October 1985.

28. M. S. Miller, "In Search of an Idealized Model of Homogeneous Solid Propellant Combustion," Combustion and Flame, Vol. 46, pp. 51-73, 1982.

29. M. S. Miller and T. P. Coffee, "A Fresh Look at the Classical Approach to Homogeneous Solid Propellant Combustion Modeling," Combustion and Flame, Vol. 50, pp. 65-74, 1983.

30. M. S. Miller and T. P. Coffee, "On the Numerical Accuracy of Homogeneous Solid Propellant Combustion Models," Combustion and Flame, Vol. 50, pp. 75-88, 1983.

31. T. P. Coffee, A. J. Kotlar, and M. S. Miller, "Applicability of the Overall Reaction Concept to Propellant Combustion," Proceedings of the 21st JANNAF Combustion Meeting, CPIA Publication 412, Vol II, pp. 437-444, October 1984.

32. A. J. Kotlar, M. S. Miller, and T. P. Coffee, "Effective Kinetic Parameters for Gas Phase Heat Release During Solid Propellant Combustion," Proceedings of the 21st JANNAF Combustion Meeting, CPIA Publication 412, Vol II, pp. 445-455, October 1984.

APPENDIX

XNOVAK Input Data Decks

```
NAME OF DATA FILE:  BASE3
BASE DECK FOR ENTIRE STUDY; 3 BURN-RATE SEGMENTS

LOVA XM39 LOTA2-202 M489 PROJECTILE
TFFFTTT          1     001
   17 3500    0 3500          .0001
0.05       188.       .0001     2.         .05        .01        .0002      .0001
    6    2    2    4    0    0    1    3    0    0    0    2

500.       14.7       29.        1.4
500.
LOVA XM39 LOTA2-202 0.         21.622     13.350     .05845
    9  .306     .015      .340      19.
17400.     .5         50000.                .5
6000.      .00006457 1.109      20000.     .006682    .5757      100000.    .0000203
1.161      0.         858.       .0277      .0001345   .6
15250000. 21.169     1.28120    28.44
9997000.  29.82       1.2254    16.78
0.         .004
3.         11.
4.41       4.41
0.         0.
0.         2.00       3.00       2.50       18.50      2.41       21.50      2.07
24.90      2.097      210.5      2.097
21.622     100.       22.622     2000.      24.5       500.       210.5      500.
21.622     23.2       44.        9.9
0.         21.622
    4    0    0
LOVA-F     G 3498.    4481.      28.64      20.954     0.0        0.0
BENITE     G 2867.5   3513.8     23.23      29.82      0.0        0.0
BENITE     S 2867.5   2867.5     0.0        0.0        0.06       .000
AIR        G 1604.89  2246.85    26.68      28.896     0.0        0.0
15250000. 1.0         0.0        0.0        0.0
9997373.   0.0        1.0        0.0        0.0
882690.    0.0        0.0        0.0        1.0
```

```
NAME OF DATA FILE:  BASE5
USED IN IGNITER OUTPUT PARTITIONING STUDIES

LOVA XM39 LOTA2-202 M489 PROJECTILE
TFFFTTT          1     001
   17 3500     0 3500          .0001
0.05       188.       .0001      2.         .05        .01        .0002      .0001
    6     2     2     4     0     0     1     3     0     0     0     2

500.       14.7       29.        1.4
500.
LOVA XM39 LOTA2-202 0.         21.622     13.350     .05845
    9  .306      .015       .340       19.
17400.     .5         50000.               .5
6000.      .00006457  1.109      20000.     .006682    .5757      100000.    .0000203
1.161      0.         858.       .0277      .0001345   .6
15250000.  21.169     1.28120    28.44
9997000.   29.82      1.2254     16.78
0.         .004
3.         11.
4.41       4.41
0.         0.
0.         2.00       3.00       2.50       18.50      2.41       21.50      2.07
24.90      2.097      210.5      2.097
21.622     100.       22.622     2000.      24.5       500.       210.5      500.
21.622     23.2       44.        9.9
0.         21.622
    4     0     0
LOVA-F     G 3498.    4481.      28.64      20.954     0.0        0.0
BENITE     G 2867.5   3513.8     23.23      29.82      0.0        0.0
BENITE     S 2867.5   2867.5     0.0        0.0        0.06       .00001
AIR        G 1604.89  2246.85    26.68      28.896     0.0        0.0
15250000.  1.0        0.0        0.0        0.0
9997373.   0.0        0.5        0.5        0.0
882690.    0.0        0.0        0.0        1.0
```

```
NAME OF DATA FILE:  BASE6
ONE GAS-PHASE REACTION

LOVA XM39 LOTA2-202 M489 PROJECTILE
TFFFTTT          1      01
   17 3500    0 3500          .0001
0.05      188.      .0001     2.        .05       .01       .0002     .0001
    6    2    2    4    0    0    1    3    0    0    0    2

500.      14.7      29.       1.4
500.
LOVA XM39 LOTA2-202 0.        21.622    13.350    .05845
    9  .306     .015      .340      19.
17400.    .5        50000.              .5
6000.     .00006457 1.109     20000.    .006682   .5757     100000.   .0000203
1.161     0.        858.      .0277     .0001345  .6
15250000. 21.169    1.28120   28.44
9997000.  29.82     1.2254    16.78
0.        .004
3.        11.
4.41      4.41
0.        0.
0.        2.00      3.00      2.50      18.50     2.41      21.50     2.07
24.90     2.097     210.5     2.097
21.622    100.      22.622    2000.     24.5      500.      210.5     500.
21.622    23.2      44.       9.9
0.        21.622
    5    1    0
LOVA-I    G 3498.   4481.     28.64     20.954    0.0       0.0
BENITE    G 2867.5  3513.8    23.23     29.82     0.0       0.0
BENITE    S 2867.5  2867.5    0.0       0.0       0.06      .000
AIR       G 1604.89 2246.85   26.68     28.896    0.0       0.0
LOVA-F    G 3498.   4481.     28.64     20.954    0.0       0.0
 7625000. 1.0       0.0       0.0       0.0
9997373.  0.0       1.0       0.0       0.0
882690.   0.0       0.0       0.0       1.0
    1    0    0    0    5    0    0    0
1.0         0.0       0.0         0.0         1.0         0.0         0.0         0.0
  7625000.    0.9E08        0.0    3.0E08        1.0         0.0         0.0
1.0
```

```
NAME OF DATA FILE:  BASE7
TWO GAS PHASE REACTIONS

LOVA XM39 LOTA2-202 M489 PROJECTILE
TFFFTTT          1      01
   17 3500    0 3500          .0001
0.05      188.      .0001     2.        .05       .01       .0002     .0001
    6    2    2    4    0    0    1    3    0    0    0    2

500.      14.7      29.       1.4
500.
LOVA XM39 LOTA2-202 0.        21.622    13.350    .05845
    9  .306     .015      .340      19.
17400.    .5        50000.              .5
6000.     .00006457 1.109     20000.    .006682   .5757     100000.   .0000203
1.161     0.        858.      .0277     .0001345  .6
15250000. 21.169    1.28120   28.44
9997000.  29.82      1.2254  16.78
0.        .004
3.        11.
4.41      4.41
0.        0.
0.        2.00      3.00      2.50      18.50     2.41      21.50     2.07
24.90     2.097     210.5     2.097
21.622    100.      22.622    2000.     24.5      500.      210.5     500.
21.622    23.2      44.       9.9
0.        21.622
    5    2    0
LOVA-I    G 3498.   4481.     28.64     20.954    0.0       0.0
BENITE    G 2867.5  3513.8    23.23     29.82     0.0       0.0
BENITE    S 2867.5  2867.5    0.0       0.0       0.06      .000
AIR       G 1604.89 2246.85   26.68     28.896    0.0       0.0
LOVA-F    G 3498.   4481.     28.64     20.954    0.0       0.0
 7625000. 1.0       0.0       0.0       0.0
9997373.  0.0       1.0       0.0       0.0
882690.   0.0       0.0       0.0       1.0
    1    0    0    0    5    0    0    0
1.0         0.0       0.0       0.0       1.0       0.0       0.0       0.0
  7625000.    0.15E8       0.0    3.0E08       1.0       0.0       0.0
1.0
    1    2    0    0    5    2    0    0
1.0         1.0       0.0       0.0       1.0       1.0       0.0       0.0
  7625000.    0.3E08       0.0    3.0E08       1.0       1.0       0.0
0.0
```

XNOVAK VERSION NUMBER 1.0024 BASE 7 ECHO

CONTROL DATA

LOGICAL VARIABLES:
PRINT T DISK WRITE F DISK READ F
I.B. TABLE T FLAME TABLE T PRESSURE TABLE(S) T
EROSIVE EFFECT 0 WALL TEMPERATURE CALCULATION 0
BED PRECOMPRESSED 0
HEAT LOSS CALCULATION 0

BORE RESISTANCE FUNCTION 1
CONSERVATIVE SCHEME TO INTEGRATE SOLID-PHASE CONTINUITY EQUATION (0=NO,OLD; 1=YES,NEW) 0
KINETICS MODE (0=NONE;1=GAS-PHASE ONLY;2=BOTH PHASES) 1

INTEGRATION PARAMETERS

NUMBER OF STATIONS AT WHICH DATA ARE STORED	17
NUMBER OF STEPS BEFORE LOGOUT	3500
TIME STEP FOR DISK START	0
NUMBER OF STEPS FOR TERMINATION	3500
TIME INTERVAL BEFORE LOGOUT(SEC)	.1000E-03
TIME FOR TERMINATION (SEC)	.5000E-01
PROJECTILE TRAVEL FOR TERMINATION (INS)	188.00
MAXIMUM TIME STEP (SEC)	.1000E-03
STABILITY SAFETY FACTOR	2.00
SOURCE STABILITY FACTOR	.0500
SPATIAL RESOLUTION FACTOR	.0100
TIME INTERVAL FOR I.B. TABLE STORAGE(SEC)	.2000E-03
TIME INTERVAL FOR PRESSURE TABLE STORAGE (SEC)	.1000E-03

FILE COUNTERS

NUMBER OF STATIONS TO SPECIFY TUBE RADIUS	6
NUMBER OF TIMES TO SPECIFY PRIMER DISCHARGE	2
NUMBER OF POSITIONS TO SPECIFY PRIMER DISCHARGE	2
NUMBER OF ENTRIES IN BORE RESISTANCE TABLE	4
NUMBER OF ENTRIES IN WALL TEMPERATURE TABLE	0
NUMBER OF ENTRIES IN FORWARD FILLER ELEMENT TABLE	0
NUMBER OF TYPES OF PROPELLANTS	1
NUMBER OF BURN RATE DATA SETS	3
NUMBER OF ENTRIES IN VOID FRACTION TABLE(S)	0 0 0
NUMBER OF ENTRIES IN PRESSURE HISTORY TABLES	2
NUMBER OF ENTRIES IN REAR FILLER ELEMENT TABLE	0

GENERAL PROPERTIES OF INITIAL AMBIENT GAS

INITIAL TEMPERATURE (DEG.R)	500.0
INITIAL PRESSURE (PSI)	14.7
MOLECULAR WEIGHT (LBM/LBMOL)	29.000
RATIO OF SPECIFIC HEATS	1.4000

GENERAL PROPERTIES OF PROPELLANT BED

INITIAL TEMPERATURE (DEG.R)	500.0

PROPERTIES OF PROPELLANT 1

PROPELLANT TYPE	LOVA XM39 LOTA2-202
MASS OF PROPELLANT (LBM)	13.3500
DENSITY OF PROPELLANT (LBM/IN**3)	.0585
FORM FUNCTION INDICATOR	9
OUTSIDE DIAMETER (INS)	.3060
INSIDE DIAMETER (INS)	.0150
LENGTH (INS)	.3400
NUMBER OF PERFORATIONS	19.

RHEOLOGICAL PROPERTIES

SPEED OF COMPRESSION WAVE IN SETTLED BED (IN/SEC)	17400.
SETTLING POROSITY	.5000
SPEED OF EXPANSION WAVE (IN/SEC)	50000.
POISSON RATIO (-)	.5000

SOLID PHASE THERMOCHEMISTRY

MAXIMUM PRESSURE FOR BURN RATE DATA (LBF/IN**2)	6000.
BURNING RATE PRE-EXPONENTIAL FACTOR (IN/SEC/PSI**BN)	.6457E-04
BURNING RATE EXPONENT	1.1090
MAXIMUM PRESSURE FOR BURN RATE DATA (LBF/IN**2)	20000.
BURNING RATE PRE-EXPONENTIAL FACTOR (IN/SEC/PSI**BN)	.6682E-02
BURNING RATE EXPONENT	.5757
MAXIMUM PRESSURE FOR BURN RATE DATA (LBF/IN**2)	100000.
BURNING RATE PRE-EXPONENTIAL FACTOR (IN/SEC/PSI**BN)	.2030E-04
BURNING RATE EXPONENT	1.1610
BURNING RATE CONSTANT (IN/SEC)	0.0000
IGNITION TEMPERATURE (DEG.R)	858.0
THERMAL CONDUCTIVITY (LBF/SEC/DEG.R)	.2770E-01
THERMAL DIFFUSIVITY (IN**2/SEC)	.1345E-03
EMISSIVITY FACTOR	.600

GAS PHASE THERMOCHEMISTRY

CHEMICAL ENERGY RELEASED IN BURNING(LBF-IN/LBM)	.15250E+08
MOLECULAR WEIGHT (LBM/LBMOL)	21.1690
RATIO OF SPECIFIC HEATS	1.2812
COVOLUME	28.4400

LOCATION OF PACKAGE(S)

PACKAGE	LEFT BODY(INS)	RIGHT BODY(INS)	MASS(LBM)
1	0.000	21.622	13.350

PROPERTIES OF PRIMER

CHEMICAL ENERGY RELEASED IN BURNING(LBF·IN/LBM)	.9997E+07
MOLECULAR WEIGHT (LBM/LBMOL)	29.8200
RATIO OF SPECIFIC HEATS	1.2254
SPECIFIC VOLUME OF SOLID(IN**3/LBM)	16.7800

PRIMER DISCHARGE FUNCTION (LBM/IN/SEC)

POS.(INS)	3.00	11.00
TIME(SEC)		
0.	4.41	4.41
.400E-02	0.00	0.00

PARAMETERS TO SPECIFY TUBE GEOMETRY

DISTANCE(IN)	RADIUS(IN)
0.000	2.000
3.000	2.500
18.500	2.410
21.500	2.070
24.900	2.097
210.500	2.097

BORE RESISTANCE TABLE

POSITION(INS)	RESISTANCE(PSI)
21.622	100.
22.622	2000.
24.500	500.
210.500	500.

THERMAL PROPERTIES OF TUBE

THERMAL CONDUCTIVITY (LBF/SEC/DEG.R)	0.
THERMAL DIFFUSIVITY (IN**2/SEC)	0.
EMISSIVITY FACTOR	0.000
INITIAL TEMPERATURE (DEG.R)	500.00

PROJECTILE AND RIFLING DATA

INITIAL POSITION OF BASE OF PROJECTILE(INS)	21.622
MASS OF PROJECTILE (LBM)	23.200
POLAR MOMENT OF INERTIA (LBM·IN**2)	44.000
ANGLE OF RIFLING (DEG)	9.900

POSITIONS FOR PRESSURE TABLE STORAGE

0.0000 21.6220

CHEMISTRY OPTION DATA

NUMBER OF SPECIES 5
NUMBER OF GAS-PHASE REACTIONS 2
NUMBER OF SOLID-PHASE REACTIONS 0
PRESSURE THRESHOLD, PSI 0.

PROPERTIES OF SPECIES

NAME	PHASE	CV LBF-IN/LBM	CP LBF-IN/LBM	COVOLUME IN**3/LBM	MOL.WGT LB/LBMOL	DENSITY LBM/IN**3	TRANSFER COEF.
LOVA-I	G	3498.0	4481.0	28.640	20.954	0.00000	0.
BENITE	G	2867.5	3513.8	23.230	29.820	0.00000	0.
BENITE	S	2867.5	2867.5	0.000	0.000	.06000	0.
AIR	G	1604.9	2246.9	26.680	28.896	0.00000	0.
LOVA-F	G	3498.0	4481.0	28.640	20.954	0.00000	0.

COMPOSITION OF LOCAL COMBUSTION PRODUCTS OF PROPELLANT 1

ENERGY	MASS FRACTIONS (-)									
LBF-IN/LBM	YO(1)	YO(2)	YO(3)	YO(4)	YO(5)	YO(6)	YO(7)	YO(8)	YO(9)	YO(10)
7625000.	1.00000	0.00000	0.00000	0.00000	0.00000					

COMPOSITION OF COMBUSTION PRODUCTS OF IGNITER

ENERGY	MASS FRACTIONS (-)									
LBF-IN/LBM	YO(1)	YO(2)	YO(3)	YO(4)	YO(5)	YO(6)	YO(7)	YO(8)	YO(9)	YO(10)
9997373.	0.00000	1.00000	0.00000	0.00000	0.00000					

COMPOSITION OF AMBIENT GAS

ENERGY	MASS FRACTIONS (-)									
LBF-IN/LBM	YO(1)	YO(2)	YO(3)	YO(4)	YO(5)	YO(6)	YO(7)	YO(8)	YO(9)	YO(10)
882690.	0.00000	0.00000	0.00000	1.00000	0.00000					

GAS-PHASE REACTION DATA

REACTION 1

REACTANT SPECIES	1	0	0	0	PRODUCT SPECIES	5	0	0	0
STOICHIOMETRIC COEFFICIENTS (LBM)	1.000	0.000	0.000	0.000		1.000	0.000	0.000	0.000
HEAT OF REACTION (LBF-IN/LBM)			7625000.						
RATE COEFFICIENT (UNITS YIELD LBM/IN**3/SEC)			.150E+08						
RATE TEMPERATURE EXPONENT (-)			0.000						
RATE ACTIVATION ENERGY (LBF-IN/LBMOL)			300000000.000						
REACTION ORDER WITH RESPECT TO REACTANTS (-)	1.000	0.000	0.000	0.000	1.000				

REACTION 2

REACTANT SPECIES	1	2	0	0	PRODUCT SPECIES	5	2	0	0
STOICHIOMETRIC COEFFICIENTS (LBM)	1.000	1.000	0.000	0.000		1.000	1.000	0.000	0.000
HEAT OF REACTION (LBF-IN/LBM)			7625000.						
RATE COEFFICIENT (UNITS YIELD LBM/IN**3/SEC)			.300E+08						
RATE TEMPERATURE EXPONENT (-)			0.000						
RATE ACTIVATION ENERGY (LBF-IN/LBMOL)			300000000.000						
REACTION ORDER WITH RESPECT TO REACTANTS (-)	1.000	1.000	0.000	0.000	0.000				

NOVSUB ERROR MESSAGE... SETTLING POROSITY AT REFERENCE COMPOSITION HAS BEEN DEFAULTED TO .41323 TO AVOID INITIAL BED COMPACTION OF PROPELLANT TYPE 1

EQUIVALENT INTBAL DATA

PROJECTILE TRAVEL(IN)	188.000
CHAMBER VOLUME(IN**3)	390.450
GUN MASS(LBM)	.100E+21
GUN RES. FAC.	0.000
ELEV. ANGLE(DEG)	0.000
PROJECTILE MASS(LBM)	23.505

PROJECTILE TRAV. (IN)	RESISTANCE(PSI)
0.000	100.000
1.000	2000.000
2.878	500.000
188.878	500.000

VEL. THRESHOLD FOR DYN. RES.(F/S)	27.000
VEL. DEPENDENCE ON CHARGE WEIGHT(F/S/LBM)	0.000
ESTIMATED MUZZLE VELOCITY(F/S)	0.000
N.B. USE VALUE FROM SUMMARY TABLE. INTBAL WILL NOT ACCEPT ZERO	
BORE AREA(IN**2)	13.815
AIR DENSITY(LBM/FT**3)	0.000
IGNITER MASS(LBM)	.0715
FLAME TEMPERATURE(K)	2012.402
RATIO OF SPECIFIC HEATS(-)	1.2254
IMPETUS(LBF-IN/LBM)	2253323.8

INITIAL CHARGE WEIGHT(LBM)	13.350
FINAL CHARGE WEIGHT(LBM)	13.350
CHARGE WEIGHT INCREMENT(LBM)	1.000
FLAME TEMPERATURE(K)	2718.749
RATIO OF SPECIFIC HEATS(-)	1.2812
IMPETUS(LBF-IN/LBM)	4288300.0
INITIAL TEMPERATURE(K)	277.8
DENSITY(LBM/IN**3)	.05845
COVOLUME(IN**3/LBM)	28.440

COEFF(IN/S/PSI**N)	EXPONENT(-)	UPPER PRES. LIM. (PSI)
.6457E-04	1.109	6000.
.6682E-02	.5757	.2000E+05
.2030E-04	1.161	.1000E+06

LENGTH OF GRAIN(IN)	.3400
EXTERNAL DIAMETER(IN)	.3060
CENTER PERF. DIAMETER(IN)	.0150
OUTER PERF. DIAMETER(IN)	.0150
DIST. BETWEEN PERF. CENTERS(IN)	.0803
OFFSET(IN)	0.0000
ANGLE(DEG)	0.0000

INTEGRATION STEP(MSEC)	.2500
PRINT STEP(MSEC)	1.0000

DISTRIBUTION LIST

No. of Copies	Organization
12	Administrator Defense Technical Info Center ATTN: DTIC-FOAC Cameron Station, Bldg 5 Alexandria, VA 22304-6145
1	Commander USA Concepts Analysis Agency ATTN: D. Hardison 8120 Woodmont Avenue Bethesda, MD 20014-2797
1	HQDA/DAMA-ZA Washington, DC 20310-2500
1	HQDA, DAMA-CSM, Washington, DC 20310-2500
1	HQDA/SARDA Washington, DC 20310-2500
1	Commander US Army War College ATTN: Library-FF229 Carlisle Barracks, PA 17013
1	US Army Ballistic Missile Defense Systems Command Advanced Technology Center P. O. Box 1500 Huntsville, AL 35807-3801
1	Chairman DOD Explosives Safety Board Room 856-C Hoffman Bldg. I 2461 Eisenhower Avenue Alexandria, VA 22331-9999
1	Commander US Army Materiel Command ATTN: AMCPM-GCM-WF 5001 Eisenhower Avenue Alexandria, VA 22333-5001
1	Commander US Army Materiel Command ATTN: AMCDRA-ST 5001 Eisenhower Avenue Alexandria, VA 22333-5001
1	Commander US Army Materiel Command ATTN: AMCDE-DW 5001 Eisenhower Avenue Alexandria, VA 22333-5001
5	Project Manager Cannon Artillery Weapons System, ARDC, AMCCOM ATTN: AMCPM-CW, F. Menke AMCPM-CWW AMCPM-CWS M. Fisette AMCPM-CWA R. DeKleine H. Hassmann Dover, NJ 07801-5001
2	Project Manager Munitions Production Base Modernization and Expansion ATTN: AMCPM-PBM, A. Siklosi AMCPM-PBM-E, L. Laibson Dover, NJ 07801-5001
3	Project Manager Tank Main Armament System ATTN: AMCPM-TMA, K. Russell AMCPM-TMA-105 AMCPM-TMA-120 Dover, NJ 07801-5001
1	Commander US Army Watervliet Arsenal ATTN: SARWV-RD, R. Thierry Watervliet, NY 12189-5001
1	Commander U.S. Army ARDEC ATTN: SMCAR-TSS Dover, NJ 07801-5001
1	Commander U.S. Army ARDEC ATTN: SMCAR-TDC Dover, NJ 07801-5001
4	Commander US Army Armament Munitions and Chemical Command ATTN: AMSMC-IMP-L Rock Island, IL 61299-7300
1	HQDA DAMA-ART-M Washington, DC 20310-2500
1	Commander US Army AMCCOM ARDEC OCAC ATTN: SMCAR-LCB-TL Benet Weapons Laboratory Watervliet, NY 12189-4050

DISTRIBUTION LIST

No. of Copies	Organization
3	Commander US Army ARDEC ATTN: SMCAR-MSI SMCAR-TDC SMCAR-LC LTC N. Barron Dover, NJ 07801-5001
7	Commander US Army ARDEC ATTN: SMCAR-LCA A. Beardell D. Downs S. Einstein S. Westley S. Bernstein C. Roller J. Rutkowski Dover, NJ 07801-5001
3	Commander US Army ARDEC ATTN: SMCAR-LCB-I D. Spring SMCAR-LCE SMCAR-LCM-E S. Kaplowitz Dover, NJ 07801-5001
4	Commander US Army ARDEC ATTN: SMCAR-LCS SMCAR-LCU-CT E. Barrieres R. Davitt SMCAR-LCU-CV C. Mandala Dover, NJ 07801-5001
3	Commander US Army ARDEC ATTN: SMCAR-LCW-A M. Salsbury SMCAR-SCA L. Stiefel B. Brodman Dover, NJ 07801-5001
1	Commander US Army Aviation Systems Command ATTN: AMSAV-ES 4300 Goodfellow Blvd. St. Louis, MO 63120-1798
1	Commander US Army TSARCOM 4300 Goodfellow Blvd. St. Louis, MO 63120-1702
1	Director US Army Aviation Research and Technology Activity Ames Research Center Moffett Field, CA 94035-1099
1	Commander US Army Communications - Electronics Command ATTN: AMSEL-ED Fort Monmouth, NJ 07703-5301
1	Commander CECOM R&D Technical Library ATTN: AMSEL-M-L (Report Section) B.2700 Fort Monmouth, NJ 07703-5000
1	Commander US Army Harry Diamond Lab. ATTN: DELHD-TA-L 2800 Powder Mill Road Adelphi, MD 20783-1145
1	Commander US Army Missile Command ATTN: AMSMI-RX M.W. Thauer Redstone Arsenal, AL 35898-5249
1	Commander US Army Missile and Space Intelligence Center ATTN: AIAMS-YDL Redstone Arsenal, AL 35898-5500
1	Commander US Army Missile Command Research, Development, and Engineering Center ATTN: AMSMI-RD Redstone Arsenal, AL 35898-5245
1	Commandant US Army Aviation School ATTN: Aviation Agency Fort Rucker, AL 36360
1	Commander US Army Tank Automotive Command ATTN: AMSTA-TSL Warren, MI 48397-5000

DISTRIBUTION LIST

No. of Copies	Organization
1	Commander US Army Tank Automotive Command ATTN: AMSTA-CG Warren, MI 48397-5000
1	Project Manager Improved TOW Vehicle ATTN: AMCPM-ITV US Army Tank Automotive Command Warren, MI 48397-5000
2	Program Manager M1 Abrams Tank System ATTN: AMCPM-GMC-SA, T. Dean Warren, MI 48092-2498
1	Project Manager Fighting Vehicle Systems ATTN: AMCPM-FVS Warren, MI 48092-2498
1	President US Army Armor & Engineer Board ATTN: ATZK-AD-S Fort Knox, KY 40121-5200
1	Project Manager M-60 Tank Development ATTN: AMCPM-M60TD Warren, MI 48092-2498
1	Director US Army TRADOC Systems Analysis Activity ATTN: ATAA-SL White Sands Missile Range, NM 88002
1	Commander US Army Training & Doctrine Command ATTN: ATCD-MA/ MAJ Williams Fort Monroe, VA 23651
2	Commander US Army Materials and Mechanics Research Center ATTN: AMXMR-ATL Tech Library Watertown, MA 02172
1	Commander US Army Research Office ATTN: Tech Library P. O. Box 12211 Research Triangle Park, NC 27709-2211
1	Commander US Army Belvoir Research and Development Center ATTN: STRBE-WC Fort Belvoir, VA 22060-5606
1	Commander US Army Logistics Mgmt Ctr Defense Logistics Studies Fort Lee, VA 23801
1	Commandant US Army Infantry School ATTN: ATSH-CD-CS-OR Fort Benning, GA 31905-5400
1	President US Army Artillery Board Ft. Sill, OK 73503-5600
1	Commandant US Army Command and General Staff College Fort Leavenworth, KS 66027
1	Commandant US Army Special Warfare School ATTN: Rev & Tng Lit Div Fort Bragg, NC 28307
3	Commander Radford Army Ammunition Plant ATTN: SMCRA-QA/HI LIB Radford, VA 24141-0298
1	Commander US Army Foreign Science & Technology Center ATTN: AMXST-MC-3 220 Seventh Street, NE Charlottesville, VA 22901-5396
2	Commandant US Army Field Artillery Center & School ATTN: ATSF-CO-MW, B. Willis Ft. Sill, OK 73503-5600
1	Commander US Army Development and Employment Agency ATTN: MODE-ORO Fort Lewis, WA 98433-5099
1	Office of Naval Research ATTN: Code 473, R. S. Miller 800 N. Quincy Street Arlington, VA 22217-9999

DISTRIBUTION LIST

No. of Copies	Organization
3	Commandant US Army Armor School ATTN: ATZK-CD-MS M. Falkovitch Armor Agency Fort Knox, KY 40121-5215
2	Commander Naval Sea Systems Command ATTN: SEA 62R SEA 64 Washington, DC 20362-5101
1	Commander Naval Air Systems Command ATTN: AIR-954-Tech Lib Washington, DC 20360
1	Assistant Secretary of the Navy (R, E, and S) ATTN: R. Reichenbach Room 5E787 Pentagon Bldg. Washington, DC 20350
1	Naval Research Lab Tech Library Washington, DC 20375
5	Commander Naval Surface Weapons Center ATTN: Code G33, J. L. East W. Burrell J. Johndrow Code G23, D. McClure Code DX-21 Tech Lib Dahlgren, VA 22448-5000
2	Comander US Naval Surface Weapons Center ATTN: J. P. Consaga C. Gotzmer Indian Head, MD 20640-5000
4	Commander Naval Surface Weapons Center ATTN: S. Jacobs/Code 240 Code 730 K. Kim/Code R-13 R. Bernecker Silver Spring, MD 20903-5000
2	Commanding Officer Naval Underwater Systems Center Energy Conversion Dept. ATTN: CODE 5B331, R. S. Lazar Tech Lib Newport, RI 02840
4	Commander Naval Weapons Center ATTN: Code 388, R. L. Derr C. F. Price T. Boggs Info. Sci. Div. China Lake, CA 93555-6001
2	Superintendent Naval Postgraduate School Dept. of Mech. Engineering Monterey, CA 93943-5100
1	Program Manager AFOSR Directorate of Aerospace Sciences ATTN: L. H. Caveny Bolling AFB, DC 20332-0001
5	Commander Naval Ordnance Station ATTN: P. L. Stang L Torreyson T. C. Smith D. Brooks Tech Library Indian Head, MD 20640-5000
1	AFSC/SDOA Andrews AFB, MD 20334
3	AFRPL/DY, Stop 24 ATTN: J. Levine/DYCR R. Corley/DYC D. Williams/DYCC Edwards AFB, CA 93523-5000
1	AFRPL/TSTL (Tech Library) Stop 24 Edwards AFB, CA 93523-5000
1	AFATL/DLYV Eglin AFB, FL 32542-5000
1	AFATL/DLXP Eglin AFB, FL 32542-5000
1	AFATL/DLJE Eglin AFB, FL 32542-5000
1	AFATL/DODL ATTN: (Tech Info Center) Eglin AFB, FL 32542-5438
1	AFWL/SUL Kirtland AFB, NM 87117

DISTRIBUTION LIST

No. of Copies	Organization
1	NASA/Lyndon B. Johnson Space Center ATTN: NHS-22, Library Section Houston, TX 77054
1	AFELM, The Rand Corporation ATTN: Library D (Required or 1700 Main Street Classified Santa Monica CA Only) 90401-3297
1	General Applied Sciences Lab ATTN: J. Erdos Merrick & Stewart Avenues Westbury Long Isld, NY 11590
2	AAI Corporation ATTN: J. Hebert J. Frankle P. O. Box 6767 Baltimore, MD 21204
1	Aerojet Ordnance Company ATTN: D. Thatcher 2521 Michelle Drive Tustin, CA 92680-7014
1	Aerojet Solid Propulsion Co. ATTN: P. Micheli Sacramento, CA 95813
1	Atlantic Research Corporation ATTN: M. K. King 5390 Cheorokee Avenue Alexandria, VA 22312-2302
1	AVCO Everett Rsch Lab ATTN: D. Stickler 2385 Revere Beach Parkway Everett, MA 02149-5936
2	Calspan Corporation ATTN: C. Morphy P. O. Box 400 Buffalo, NY 14225-0400
10	Central Intelligence Agency Office of Central Reference Dissemination Branch Room GE-47 HQS Washington, DC 20505
1	General Electric Company Armament Systems Dept. ATTN: M. J. Bulman, Room 1311 128 Lakeside Avenue Burlington, VT 05401-4985
1	IITRI ATTN: M. J. Klein 10 W. 35th Street Chicago, IL 60616-3799
1	Hercules Inc. Allegheny Ballistics Laboratory ATTN: R. B. Miller P. O. Box 210 Cumberland, MD 21501-0210
1	Hercules, Inc. Bacchus Works ATTN: K. P. McCarty P. O. Box 98 Magna, UT 84044-0098
1	Hercules, Inc. Radford Army Ammunition Plant ATTN: J. Pierce Radford, VA 24141-0299
1	Honeywell, Inc. - MN64 2200 Defense Systems Division ATTN: C. Hargreaves 6110 Blue Circle Drive Minnetonka MN 55436
1	*Lawrence Livermore National* Laboratory ATTN: L-355, A. Buckingham M. Finger P. O. Box 808 Livermore, CA 94550-0622
1	Lawrence Livermore National Laboratory ATTN: L-324/M. Constantino P. O. Box 808 Livermore, CA 94550-0622
1	Olin Corporation Badger Army Ammunition Plant ATTN: R. J. Thiede Baraboo, WI 53913
1	Olin Corporation Smokeless Powder Operations ATTN: D. C. Mann P.O. Box 222 St. Marks, FL 32355-0222
1	Paul Gough Associates, Inc. ATTN: P. S. Gough P. O. Box 1614, 1048 South St. Portsmouth, NH 03801-1614

DISTRIBUTION LIST

No. of Copies	Organization
1	Physics International Company ATTN: Library H. Wayne Wampler 2700 Merced Street San Leandro, CA 94577-5602
1	Princeton Combustion Research Lab., Inc. ATTN: M. Summerfield 475 US Highway One Monmouth Junction, NJ 08852-9650
2	Rockwell International Rocketdyne Division ATTN: BA08 J. E. Flanagan J. Gray 6633 Canoga Avenue Canoga Park, CA 91303-2703
1	Science Applications, Inc. ATTN: R. B. Edelman 23146 Cumorah Crest Drive Woodland Hills, CA 91364-3710
3	Thiokol Corporation Huntsville Division ATTN: D. Flanigan R. Glick Tech Library Huntsville, AL 35807
2	Thiokol Corporation Elkton Division ATTN: R. Biddle Tech Lib. P. O. Box 241 Elkton, MD 21921-0241
2	United Technologies Chemical Systems Division ATTN: R. Brown Tech Library P. O. Box 358 Sunnyvale, CA 94086-9998
1	Veritay Technology, Inc. ATTN: E. Fisher 4845 Millersport Hwy. P. O. Box 305 East Amherst, NY 14051-0305
1	Universal Propulsion Company ATTN: H. J. McSpadden Black Canyon Stage 1 Box 1140 Phoenix, AZ 85029
1	Battelle Memorial Institute ATTN: Tech Library 505 King Avenue Columbus, OH 43201-2693
1	Brigham Young University Dept. of Chemical Engineering ATTN: M. Beckstead Provo, UT 84601
1	California Institute of Tech 204 Karman Lab Main Stop 301-46 ATTN: F. E. C. Culick 1201 E. California Street Pasadena, CA 91109
1	California Institute of Tech Jet Propulsion Laboratory ATTN: L. D. Strand 4800 Oak Grove Drive Pasadena, CA 91109-8099
1	University of Illinois Dept of Mech/Indust Engr ATTN: H. Krier 144 MEB; 1206 N. Green St. Urbana, IL 61801-2978
1	University of Massachusetts Dept. of Mech. Engineering ATTN: K. Jakus Amherst, MA 01002-0014
1	University of Minnesota Dept. of Mech. Engineering ATTN: E. Fletcher Minneapolis, MN 55414-3368
1	Case Western Reserve University Division of Aerospace Sciences ATTN: J. Tien Cleveland, OH 44135
3	Georgia Institute of Tech School of Aerospace Eng. ATTN: B. T. Zinn E. Price W. C. Strahle Atlanta, GA 30332
1	Institute of Gas Technology ATTN: D. Gidaspow 3424 S. State Street Chicago, IL 60616-3896

DISTRIBUTION LIST

No. of Copies	Organization
1	Johns Hopkins University Applied Physics Laboratory Chemical Propulsion Information Agency ATTN: T. Christian Johns Hopkins Road Laurel, MD 20707-0690
1	Massachusetts Institute of Technology Dept of Mechanical Engineering ATTN: T. Toong 77 Massachetts Avenue Cambridge, MA 02139-4307
1	G. M. Faeth Pennsylvania State University Applied Research Laboratory University Park, PA 16802-7501
1	Pennsylvania State University Dept. Of Mech. Engineering ATTN: K. Kuo University Park, PA 16802-7501
1	Purdue University School of Mechanical Engineering ATTN: J. R. Osborn TSPC Chaffee Hall West Lafayette, IN 47907-1199
1	SRI International Propulsion Sciences Division ATTN: Tech Library 333 Ravenswood Avenue Menlo Park, CA 94025-3493
1	Rensselaer Polytechnic Inst. Department of Mathematics Troy, NY 12181
2	Director Los Alamos Scientific Lab ATTN: T3, D. Butler M Division, B. Craig P. O. Box 1663 Los Alamos, NM 87544
1	Stevens Institute of Technology Davidson Laboratory ATTN: R. McAlevy, III Castle Point Station Hoboken, NJ 07030-5907
1	Rutgers University Dept. of Mechanical and Aerospace Engineering ATTN: S. Temkin University Heights Campus New Brunswick, NJ 08903
1	University of Southern California Mechanical Engineering Dept. ATTN: 0HE200, M. Gerstein Los Angeles, CA 90089-5199
2	University of Utah Dept. of Chemical Engineering ATTN: A. Baer G. Flandro Salt Lake City, UT 84112-1194
1	Washington State University Dept. of Mech. Engineering ATTN: C. T. Crowe Pullman, WA 99163-5201

Aberdeen Proving Ground

Dir, USAMSAA
ATTN: AMXSY-D
AMXSY-MP, H. Cohen

Cdr, USATECOM
ATTN: AMSTE-SI-F
AMSTE-CM-F, L. Nealley

Cdr, CSTA
ATTN: STECS-AS-H, R. Hendricksen

Cdr, CRDC, AMCCOM
ATTN: SMCCR-RSP-A
SMCCR-MU
SMCCR-SPS-IL

USER EVALUATION SHEET/CHANGE OF ADDRESS

This Laboratory undertakes a continuing effort to improve the quality of the reports it publishes. Your comments/answers to the items/questions below will aid us in our efforts.

1. BRL Report Number _____ Date of Report _____

2. Date Report Received _____

3. Does this report satisfy a need? (Comment on purpose, related project, or other area of interest for which the report will be used.) _____

_____

_____

4. How specifically, is the report being used? (Information source, design data, procedure, source of ideas, etc.) _____

_____

_____

5. Has the information in this report led to any quantitative savings as far as man-hours or dollars saved, operating costs avoided or efficiencies achieved, etc? If so, please elaborate. _____

_____

_____

6. General Comments. What do you think should be changed to improve future reports? (Indicate changes to organization, technical content, format, etc.)

_____

_____

_____

CURRENT ADDRESS

_____
Name

_____
Organization

_____
Address

_____
City, State, Zip

7. If indicating a Change of Address or Address Correction, please provide the New or Correct Address in Block 6 above and the Old or Incorrect address below.

OLD ADDRESS

_____
Name

_____
Organization

_____
Address

_____
City, State, Zip

(Remove this sheet, fold as indicated, staple or tape closed, and mail.)

FOLD HERE

Director
US Army Ballistic Research Laboratory
ATTN: DRXBR-OD-ST
Aberdeen Proving Ground, MD 21005-5066

NO POSTAGE
NECESSARY
IF MAILED
IN THE
UNITED STATES

OFFICIAL BUSINESS
PENALTY FOR PRIVATE USE, $300

BUSINESS REPLY MAIL
FIRST CLASS PERMIT NO 12062 WASHINGTON, DC
POSTAGE WILL BE PAID BY DEPARTMENT OF THE ARMY

Director
US Army Ballistic Research Laboratory
ATTN: DRXBR-OD-ST
Aberdeen Proving Ground, MD 21005-9989

FOLD HERE